Inverse percolation by removing straight rigid rods from square lattices

J. Stat. Mech. (2015) P09003

(http://iopscience.iop.org/1742-5468/2015/9/P09003)

Journal of Statistical Mechanics: Theory and Experiment
An IOP and SISSA journal

Inverse percolation by removing straight rigid rods from square lattices

L S Ramirez, P M Centres and A J Ramirez-Pastor

Departamento de Física, Instituto de Física Aplicada, Universidad Nacional de San Luis-CONICET, Ejército de Los Andes 950, D5700HHW San Luis, Argentina
E-mail: antorami@unsl.edu.ar

Received 8 June 2015
Accepted for publication 6 August 2015
Published 8 September 2015

Online at stacks.iop.org/JSTAT/2015/P09003
doi:10.1088/1742-5468/2015/09/P09003

Abstract. Numerical simulations and finite-size scaling analysis have been carried out to study the problem of inverse percolation by removing straight rigid rods from square lattices. The process starts with an initial configuration, where all lattice sites are occupied and, obviously, the opposite sides of the lattice are connected by nearest-neighbor occupied sites. Then, the system is diluted by randomly removing straight rigid rods of length k (k-mers) from the surface. The central idea of this paper is based on finding the maximum concentration of occupied sites (minimum concentration of holes) for which connectivity disappears. This particular value of concentration is called the *inverse percolation threshold*, and determines a well-defined geometrical phase transition in the system. The results, obtained for k ranging from 2 to 256, showed a nonmonotonic size k dependence for the critical concentration, which rapidly decreases for small particle sizes ($1 \leqslant k \leqslant 3$). Then, it grows for $k = 4$, 5 and 6, goes through a maximum at $k = 7$, and finally decreases again and asymptotically converges towards a definite value for large values of k. Percolating and non-percolating phases extend to infinity in the space of the parameter k and, consequently, the model presents percolation transition in all ranges of said value. This finding contrasts with the results obtained in literature for a complementary problem, where straight rigid k-mers are randomly and irreversibly deposited on a square lattice, and the percolation transition only exists for values of k ranging between 1 and approximately 1.2×10^4. The breaking of particle-hole symmetry, a distinctive characteristic of the k-mers statistics, is the source of this asymmetric behavior. Finally, the

accurate determination of critical exponents reveals that the model belongs to the same universality class as random percolation regardless of the value of k considered.

Keywords: classical Monte Carlo simulations, classical phase transitions (theory), phase diagrams (theory), percolation problems (theory)

Contents

1. Introduction

Percolation is one of the central problems in statistical mechanics and has been attracting a great deal of interest for a long time. It settles the basis for the understanding of the behavior of many systems such as metal-insulator phase transitions, fluid flow in random media, the spread of disease in populations, forest fire propagation, sol-gel transitions and failures in complex networks [1–3]. Percolation models have also been used to understand many chemical, biological, and social phenomena [2, 4, 5].

The usual setup is that of a bond or site percolation on a lattice, where each element (site or bond) is occupied with probability $\theta \in [0, 1]$ or empty (non-occupied) with probability $1 - \theta$, independently of the others. Nearest-neighbor occupied sites (bonds) form structures called clusters. The main idea of the classical percolation theory is based on finding the minimum concentration of elements for which a cluster extends from one side of the system to the other. This particular value of concentration rate is named critical concentration or percolation threshold θ_c, and determines a phase transition in the system. For $\theta < \theta_c$, almost all connected components are finite, while for $\theta > \theta_c$ a

J. Stat. Mech. (2015) P09003

large cluster emerges (infinite in the thermodynamic limit), spanning from one side of the lattice to the other. [1]. This geometric transition is a second-order phase transition and can be characterized by well-defined critical exponents.

More general percolation problems can be formulated by including the deposition of objects occupying more than one site (bond) on the lattice [6–11]. In [6], linear k-mers (particles that occupy k contiguous lattice sites) with a length in the interval $k = 1$, ..., 20 were randomly and isotropically deposited on the lattice. By computer simulations, the authors found that the percolation threshold decreases with an increase in the chain length k. Similar behavior has been observed by Cornette *et al* [7, 8] for sizes k ranging between 1 and 15. In addition, an exhaustive calculation of critical exponents reveals that the problem belongs to the random percolation universality class no matter the size of k used in the experiment.

Leroyer and Pommiers [9] extended the study of linear k-mers on square lattices to larger particle sizes (k values up to 40) and found that the percolation threshold initially decreases, goes through a minimum around $k = 13$–15, and then increases as the length of the segments increases. The behavior reported in [9] was corroborated by Kondrat and Pekalski [10], who studied the same problem in the interval $k = 1 \ldots 2000$. However, large finite-size corrections are expected for very large values of k because of the moderate size of the studied lattices ($L \leqslant 2500$).

Recently, percolation of partially ordered linear k-mers on square lattices has been intensively studied for values of k varying from 1 to 512 and lattice sizes of up to $L = 1024k$ [11]. In the case of isotropic systems, Tarasevich *et al* confirmed that the percolation threshold initially decreases, passes through a minimum at $k = 13$, and then increases with increasing k. In addition, the authors determined that the percolation phase transition only exists for values of k ranging between 1 and approximately 1.2×10^4. For $k > 1.2 \times 10^4$, percolation can not occur even at (maximal) jamming concentration.

Percolation theory can also be used to describe the response of the network to the removal of nodes or links, the phenomena of primary interest in robustness [12]. From this point of view, we can think of a regular lattice as a network whose nodes (sites or bonds) are occupied. Then, a fraction θ^* of elements (sites or bonds) is removed, with the aim of finding out how their absence impacts the integrity of the lattice. If θ^* is small, the few missing nodes do little damage to the network. As θ^* is increased above a certain critical value θ_c^*, the initial large cluster breaks into tiny non-communicating components and connectivity between both sides of the lattice disappears. The mathematical model of such a process can be thought of as an inverse percolation process [13].

An analogous problem can be formulated for continuum percolation, where the system is not restricted to a lattice. In this case, one considers a system of overlapping objects (spheres, ellipses, etc) and asks when the space not occupied by the objects percolates. This topic is known as void percolation or Swiss-cheese percolation [14–18].

The study of robustness as an inverse percolation problem is important for many fields [13]. In ecology, robustness is an important attribute of ecosystems [19]. For biologists, network robustness can help in the study of diseases and mutations [20]. In communications and information theory, it can be used to find out what fraction of Internet routers must break down so that the Internet turns into isolated clusters of computers that are unable to communicate with each other [21, 22], etc.

J. Stat. Mech. (2015) P09003

When single nodes (sites or bonds) are perturbed (deleted), the fragmentation process is not gradual and a second-order phase transition occurs at a critical value of the concentration of deleted elements θ_c^*. For $\theta^* < \theta_c^*$, an infinite cluster connects one side of the lattice to the other, but once θ^* exceeds θ_c^*, connectivity vanishes. The critical exponents characterizing this transition are the same as those encountered in classical percolation, and the two processes can be mapped to each other by choosing $\theta^* = 1 - \theta$.

The behavior described in the paragraph above is a consequence of particle-hole symmetry characterizing the usual single-particle statistics (depositing elements that occupy one single node and removing single elements). However, if some sort of correlation between the occupation probabilities of adjacent sites (bonds) is introduced, no equivalence exists between particles and vacancies, and the mapping between standard and inverse percolation is not straightforward. The objective of the present paper is to provide a thorough study in this direction. For this purpose, extensive numerical simulations supplemented by analysis using finite-size scaling theory have been carried out to study the problem of inverse percolation by removing straight rigid rods from square lattices. Our interest is in characterizing the phase transition occurring (or not) in the system and in comparing the results obtained with those reported for the complementary problem, where straight rigid k-mers are randomly and irreversibly deposited on a square lattice [6–11].

It is quite obvious that the system considered here is highly idealized and is not meant to reproduce a particular experiment. However, the model offers a simplified representation of an irreversible reaction-annihilation process [23, 24]. In fact, we can think of a set of k nearest-neighbor particles which react and desorb from the surface, leaving behind k holes ($A^{(1)} + A^{(2)} + \cdots + A^{(k)} \to 0$). This point could be an interesting topic for further research.

This paper is organized as follows: the model and the simulation scheme are described in sections 2 and 3, respectively. The dependence of the percolation threshold on the size k of the objects removed from the surface is presented in section 4. The analysis of results obtained by using finite size scaling theory is discussed in section 5. The main purpose of this section is to test the universality of the problem by determining the numerical values of the critical exponents of the phase transition. Finally, conclusions are presented in section 6.

2. The model

Let us consider a square lattice of $M = L \times L$ sites and periodic boundary conditions. Each site can be empty (hole) or occupied by just one particle. Particles and holes are distributed with a concentration of θ and $\theta^*(= 1 - \theta)$, respectively. Nearest-neighbor occupied sites form structures called clusters, and the distribution of these sites determines the probability of the existence of a large cluster (also called an 'infinite' cluster, inspired by the thermodynamic limit) that connects from one side of the lattice to the other.

In the starting configuration, all lattice sites are occupied by particles ($\theta = 1$ and $\theta^* = 0$) and, obviously, the opposite sides of the lattice are connected by occupied

J. Stat. Mech. (2015) P09003

sites. Then, the system is diluted by randomly removing particles from the lattice. The procedure of dilution is as follows: (i) one of the possible (x, y) lattice directions and a starting site are randomly chosen; and (ii) if, beginning at the chosen site, there are k consecutive occupied sites (particles), then a k-mer is removed from those sites–otherwise, the attempt is rejected. When N rods are removed, the concentration of particles (holes) is $\theta = (M - kN)/M$ $(\theta^* = kN/M)$. As mentioned in the previous section, the model offers a simplified representation of an irreversible reaction-annihilation process $(A^{(1)} + A^{(2)} + \cdots + A^{(k)} \to 0)$ [23, 24]. Figure 1 shows a typical surface configuration after the removal of a fraction $\theta^* = 0.24$ of particles. In this case, the holes (empty sites, open circles) were produced by the removal of tetramers (k-mers with $k = 4$). Particles (occupied sites) are represented by solid circles.

As already mentioned, the central idea of the inverse percolation model is based on finding the minimum concentration θ^* for which connectivity disappears. This particular value of concentration is called *critical concentration* θ_c^*, and determines a well-defined geometrical phase transition in the system, where the critical concentration separates a phase where an infinite cluster is present $(\theta^* < \theta_c^*)$ from a phase of finite clusters $(\theta^* > \theta_c^*)$. This is a second-order phase transition and can be characterized by well-defined critical exponents. We will call the *inverse percolation threshold* θ_c the density of particles at the critical point $\theta_c = 1 - \theta_c^*$. Our interest is in determining (i) how the percolation threshold is modified when the size of the k-mer is increased and (ii) what universality class the phase transition of this problem belongs to.

Let us consider a mapping $L \to L^*$ from the original lattice L to the complementary lattice L^* where each empty (occupied) site of L transforms into an occupied (empty) one of L^*. Under these conditions, the filling process in the complementary lattice (dilution process in the original lattice) is equivalent to a random sequential adsorption (RSA) process of straight rigid k-mers. Accordingly, the final state in L^* is a disordered state (known as a jamming state), in which no more objects can be deposited due to the absence of free space of appropriate size and shape [25]. The corresponding limiting or jamming coverage, $\theta_{j,k}^* \equiv \theta^*(t = \infty)$ is less than that corresponding to close packing $(\theta_{j,k}^* < 1)$. Note that $\theta^*(t)$ represents the fraction of complementary lattice sites covered at time t by the deposited objects.

The jamming coverage depends on the size of the deposited object and the lattice geometry [10, 11, 25–29]. In the case of square lattices, the dependence of $\theta_{j,k}^*$ as a function of the size k has been studied by several authors [26, 30]. Among them, Bonnier *et al* [26] found that (1) $\theta_{j,k}^*$ is a decreasing function of k, and (2) the best fit to $\theta_{j,k}^*$ (obtained for $k \geqslant 48$) corresponds to the expression $\theta_{j,k}^* = 0.660 + 1.071/k - 3.47/k^2$, being $\theta_{j,\infty}^* = 0.660(2)$ the result for the coverage limit of a square lattice by infinitely long k-mers. For $2 < k < 40$, the results in [26] were corroborated by Dolz *et al* [30].

Then, during the dilution process in the original lattice, the fraction of holes varies between 0 and $\theta_{j,k}^*$, while the fraction of occupied sites ranges from 1 to $\theta_{j,k} (\equiv 1 - \theta_{j,k}^*)$ and [26]

$$\theta_{j,k} = 0.34 - \frac{1.071}{k} + \frac{3.47}{k^2} (k \geqslant 48). \tag{1}$$

J. Stat. Mech. (2015) P09003

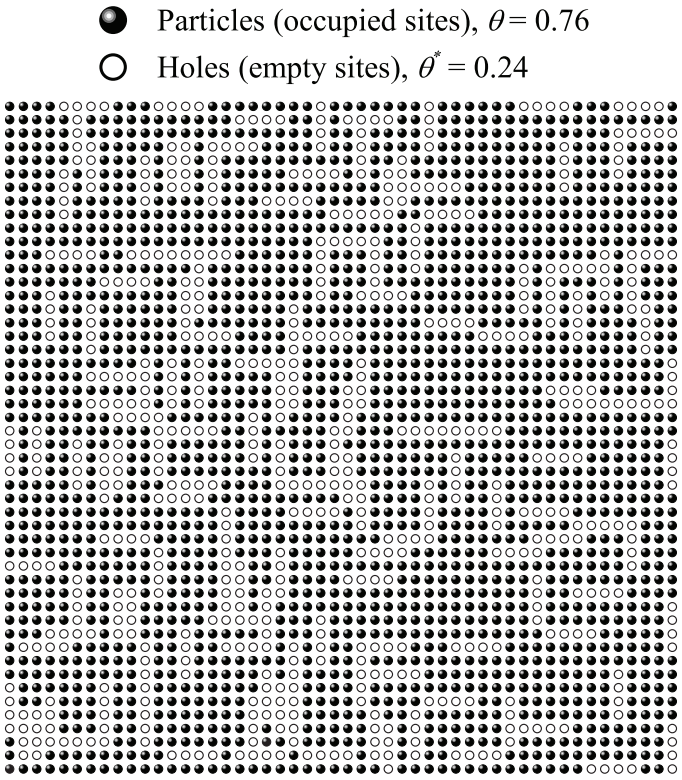

Figure 1. Typical surface configuration for $\theta = 0.76$ ($\theta^* = 0.24$). In this case, the holes (empty sites, open circles) were produced by the removal of tetramers (k-mers with $k = 4$). Particles (occupied sites) are represented by solid circles.

Now that the parameter space θ and θ^* has been determined, the percolation properties of the system will be studied in the following.

3. Simulation scheme

It is well known that it is quite a difficult matter to analytically determine the value of a percolation threshold for a given lattice [1]. For some special types of lattice, geometrical considerations enable their percolation thresholds to be derived exactly. For different conditions, i.e. for systems which do not present such a topological advantage, percolation thresholds have to be estimated numerically by means of computer simulations.

In the present case, each simulation run consists of the following two steps: (a) the construction of the lattice for the desired fraction θ of occupied sites (according to the procedure described in section 2), and (b) cluster analysis using the Hoshen and Kopelman algorithm [31]. In the last step, the size of the largest cluster S_L, as well as the existence of a percolating island, is determined. For this purpose, the probability $R^X_{L,k}(\theta)$ that a lattice composed of $L \times L$ sites percolates at the concentration θ of occupied sites can be defined [1]. The subindex k in the definition of R indicates that the

density θ was reached by removing sets of particles of size k (k-mers). Here, the following definitions can be given according to the meaning of X [32]:

- $R^R_{L,k}(\theta)$: the probability of finding a rightward percolating cluster, along the x-direction,
- $R^D_{L,k}(\theta)$: the probability of finding a downward percolating cluster, along the y-direction.

Other useful definitions for finite size analysis are:

- $R^U_{L,k}(\theta)$: the probability of finding a cluster which percolates in any direction,
- $R^I_{L,k}(\theta)$: the probability of finding a cluster which percolates in two (mutually perpendicular) directions,
- $R^A_{L,k}(\theta) = \frac{1}{2}[R^U_{L,k}(\theta) + R^I_{L,k}(\theta)]$.

A total of m_L independent runs of two such procedure steps were carried out for each lattice size L, and from these runs a number m^X_L of them present a percolating cluster. This is done for the desired criterion among $X = \{R, D, I, U, A\}$. Then, $R^X_{L,k}(\theta) = m^X_L/m_L$ is defined and the procedure is repeated for different values of L, θ and k-mer size. A set of $m_L = 10^5$ independent random samples is numerically prepared for several values of the system size ($L/k = 128, 256, 384, 512, 640$). As can be appreciated, this represents extensive calculations from the numeric point of view. From there on, the finite-scaling theory can be used to determine the percolation threshold and critical exponents with reasonable accuracy [1, 32, 33].

In addition to different probabilities $R^X_{L,k}(\theta)$, percolation order parameter ($P = \langle S_L\rangle/M$) [34, 35] has been measured, where S_L represents the size of the largest cluster and $\langle ...\rangle$ means an average over simulation runs.

The quantities related to the order parameter, such as the susceptibility χ and the reduced fourth-order cumulant U_L introduced by Binder [33], can be calculated as

$$\chi = [\langle S^2_L\rangle - \langle S_L\rangle^2]/M, \tag{2}$$

and

$$U_L = 1 - \frac{\langle S^4_L\rangle}{3\langle S^2_L\rangle^2}. \tag{3}$$

4. Percolation threshold

As already explained, percolation is determined for 10^5 runs for each concentration θ, on each lattice size L, for each k-mer size, and for each percolation criterion ($X = R$, D,

J. Stat. Mech. (2015) P09003

I, U, A). Functions $R^X_{L,k}(\theta)$ are reported in figure 2, for $k = 5$ (a), $k = 7$ (b), $k = 9$ (c) and different percolation criteria as indicated.

From a simple inspection of figure 2 (and from data not shown here for the sake of clarity), it is observed that $R^X_{L,k}$ curves cross each other at a unique point $R^{X^*}_k$, which is located at a well-defined value in the θ-axes determining the critical threshold for each k. The value of $R^{X^*}_k$ depends on the criterion X used: $R^{A^*}_k \approx 0.50$; $R^{I^*}_k \approx 0.32$ and $R^{U^*}_k \approx 0.68$. These results coincide (within the numerical errors) with the corresponding exact values for standard percolation: A criterion, $1/2$ [36, 38]; I criterion, $0.322\,120\,45\ldots$ [37, 38] and U criterion, $0.677\,889\,54\ldots$ [37, 38]. In addition, the crossing points do not modify their numerical value for the different k-sizes used (ranging between $k = 1$ to $k = 256$), presenting a first indication that the phase transition involved in the problem belongs to the ordinary percolation universality class no matter the value of k considered in the experiment.

In order to express $R^X_{L,k}(\theta)$ as a function of continuous values of θ, it is convenient to fit $R^X_{L,k}(\theta)$ with some approximating function through the least-squares method. The fitting curve is the *error function* because $\mathrm{d}R^X_{L,k}(\theta)/\mathrm{d}\theta$ is expected to behave like the Gaussian distribution[1] [32]

$$\frac{\mathrm{d}R^X_{L,k}}{\mathrm{d}\theta} = \frac{1}{\sqrt{2\pi}\,\Delta^X_{L,k}} \exp\left\{-\frac{1}{2}\left[\frac{\theta - \theta^X_{c,k}(L)}{\Delta^X_{L,k}}\right]^2\right\}, \tag{4}$$

where $\theta^X_{c,k}(L)$ is the concentration at which the slope of $R^X_{L,k}(\theta)$ is the largest and $\Delta^X_{L,k}$ is the standard deviation from $\theta^X_{c,k}(L)$.

With previous results for $\theta^X_{c,k}(L)$, a scaling analysis can be done [1]. Thus, we have

$$\theta^X_{c,k}(L) = \theta^X_{c,k}(\infty) + A^X L^{-1/\nu}, \tag{5}$$

where A^X is a non-universal constant and ν is the critical exponent of the correlation length which will be taken as $4/3$ for the present analysis, since, as will be shown in section 5, our model belongs to the same universality class as random percolation [1].

Figure 3 shows the plots towards the thermodynamic limit of $\theta^X_{c,k}(L)$ according to equation (5) for the data in figure 2. From extrapolations it is possible to obtain $\theta^X_{c,k}(\infty)$ for the criteria I, A and U. Combining the three estimates for each case, the final values of $\theta_{c,k}(\infty)$ can be obtained. Additionally, the maximum of differences between $|\theta^U_{c,k}(\infty) - \theta^A_{c,k}(\infty)|$ and $|\theta^I_{c,k}(\infty) - \theta^A_{c,k}(\infty)|$ gives the error bar for each determination of $\theta_{c,k}(\infty)$. In this case, the values obtained were: $\theta_{c,k=5}(\infty) = 0.5692(1)$, $\theta_{c,k=7}(\infty) = 0.5706(1)$ and $\theta_{c,k=9}(\infty) = 0.5688(1)$.

Figure 4 shows the behavior of U_L (equation (3)) as a function of θ for the same cases presented in figure 2. In the vicinity of the critical point, cumulants show a

[1] Even though the behavior of $\mathrm{d}R^X_{L,k}(\theta)/\mathrm{d}\theta$ is known not to be a Gaussian in all range of coverage, this quantity is approximately Gaussian near the peak, and equation (4) is a good approximation for the purpose of locating its maximum.

J. Stat. Mech. (2015) P09003

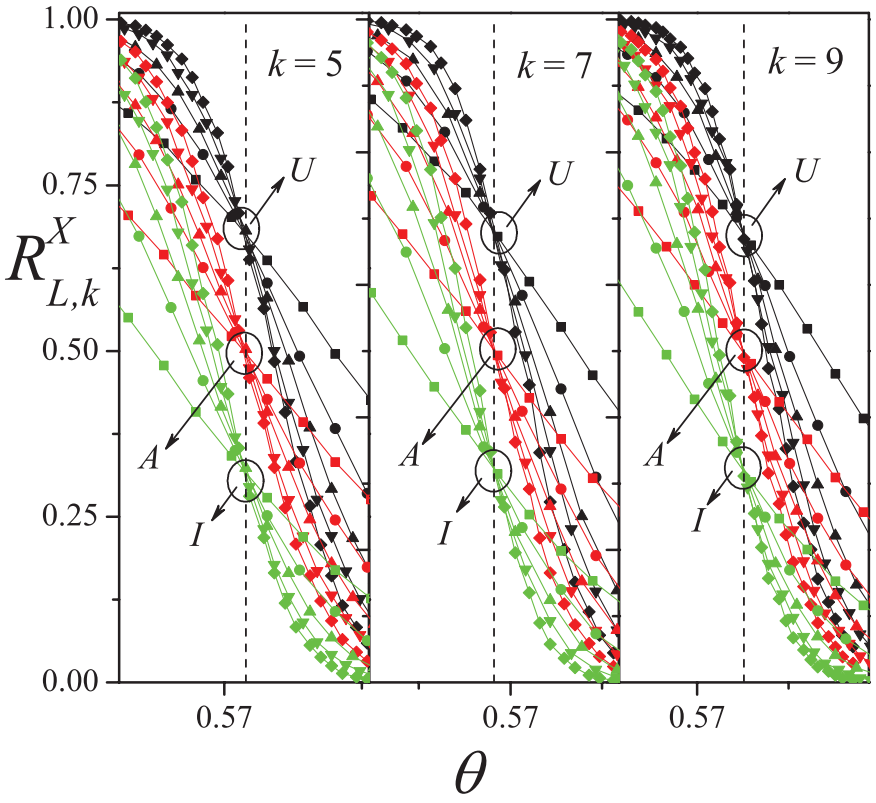

Figure 2. Fraction of percolating lattices $R^X_{L,k}(\theta)$ ($X = I$, U, A as indicated) as a function of the concentration θ for $k = 5$ (left), $k = 7$ (middle) and $k = 9$ (right) and different lattice sizes: $L/k = 128$, squares; $L/k = 256$, circles; $L/k = 384$, up triangles; $L/k = 512$, down triangles and $L/k = 640$, diamonds. The vertical dashed line denotes the percolation threshold $\theta_{c,k}$ in the thermodynamic limit.

strong dependence on the system size. However, at the critical point the cumulants adopt a constant value, irrespective of system sizes in the scaling limit. Thus, plotting $U_L(\theta)$ for different linear dimensions yields an intersection point, which allows for another efficient route for estimating critical density in the infinite system. In the case of figure 4, the values obtained for the critical density were: $\theta_{c,k=5}(\infty) = 0.5693(2)$, $\theta_{c,k=7}(\infty) = 0.5706(2)$ and $\theta_{c,k=9}(\infty) = 0.5688(3)$.

Previous work on the determination of the percolation threshold via crossing points (as in figures 2 and 4) demonstrated that those crossing points obey finite-size corrections in general [39]. The apparent lack of finite-size corrections at the crossing points in figures 2 and 4 is a consequence of statistical error and the fact that said corrections are small. Interested readers are referred to [39] for a more complete discussion on this subject.

As can be seen, there are no great differences between the results obtained from the extrapolation of $\theta^X_{c,k}(L)$ (figure 3) and those obtained from the intersection point of the cumulants (figure 4). For the rest of the paper we will use just one percolation threshold for each size k corresponding to the mean value between the results given by these two methods: $\theta_{c,k}$ (for simplicity we will drop the '(∞)').

J. Stat. Mech. (2015) P09003

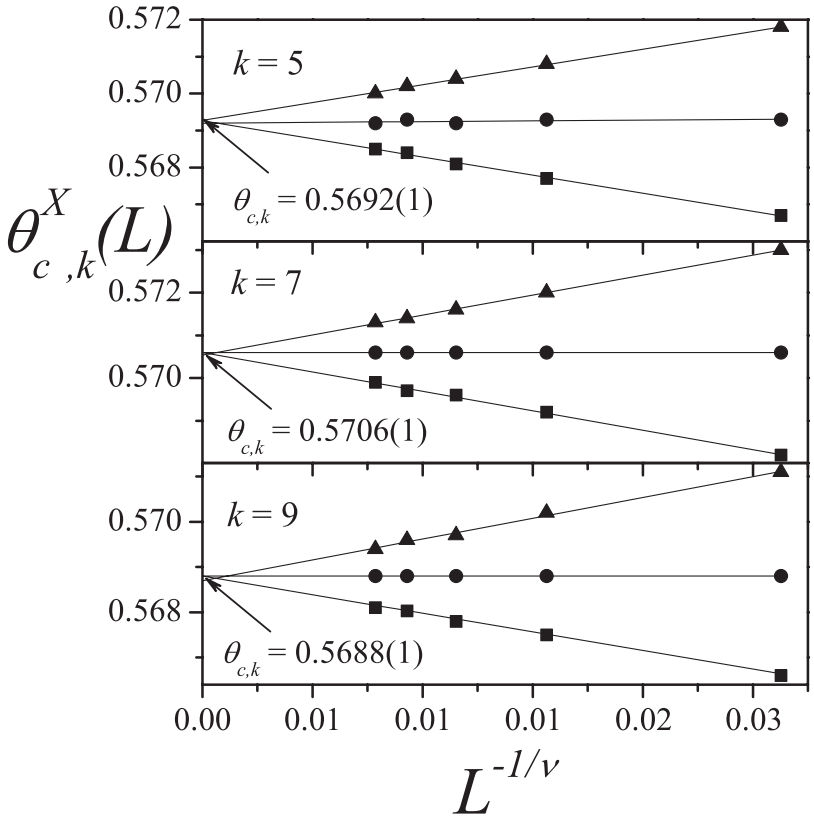

Figure 3. Extrapolation of $\theta^X_{c,k}(L)$ towards the thermodynamic limit according to the theoretical prediction given by equation (5). Triangles, circles and squares denote the values of $\theta^X_{c,k}(L)$ obtained by using the criteria I, A and U, respectively. Different values of k are presented as indicated.

The procedure of figures 3 and 4 was repeated for k ranging between 2 and 16, and the results are shown in figure 5 (solid circles) and collected in table 1. In the case of monomers ($k = 1$), the particle-hole symmetry allows us to conclude that $\theta_{c,1} \approx 0.592\,746$ (open circle in figure 5) [40]. For $k > 1$, no statistical equivalence exists between particles and vacancies and $\theta_{c,k}$ shows a nonmonotonic behavior with increasing k. To begin with, for $1 \leqslant k \leqslant 3$, the curve rapidly decreases, then it grows for $k = 4$, 5 and 6, goes through a maximum at $k = 7$, and finally decreases again for $k \geqslant 7$.

The calculations were extended up to $k = 256$. The points corresponding to $k = 20$, $k = 32$ and $k = 64$ were calculated for $L/k = 128$ and $L/k = 256$. In the case of $k = 128$ and $k = 256$, two relatively small values of L/k were used ($L/k = 64$ and $L/k = 128$), with an effort almost reaching the limits of our computational capabilities. The results are shown in figure 6(a) (solid circles) and a compilation of the numerical values is also presented in table 1.

As can be observed from figure 6(a), $\theta_{c,k}$ is a monotonically decreasing function of k in the interval $(7, \infty)$. The decrease of $\theta_{c,k}$ for large values of k could be fitted by a two-exponential function. The best fit according to this behavior, realized for $k \geqslant 10$, allows us to obtain the value of the percolation threshold as $k \to \infty$: $\theta_{c,\infty} = 0.454(4)$. The corresponding fitting curve is shown in figure 6(b) for k in the range 10^3–10^4.

J. Stat. Mech. (2015) P09003

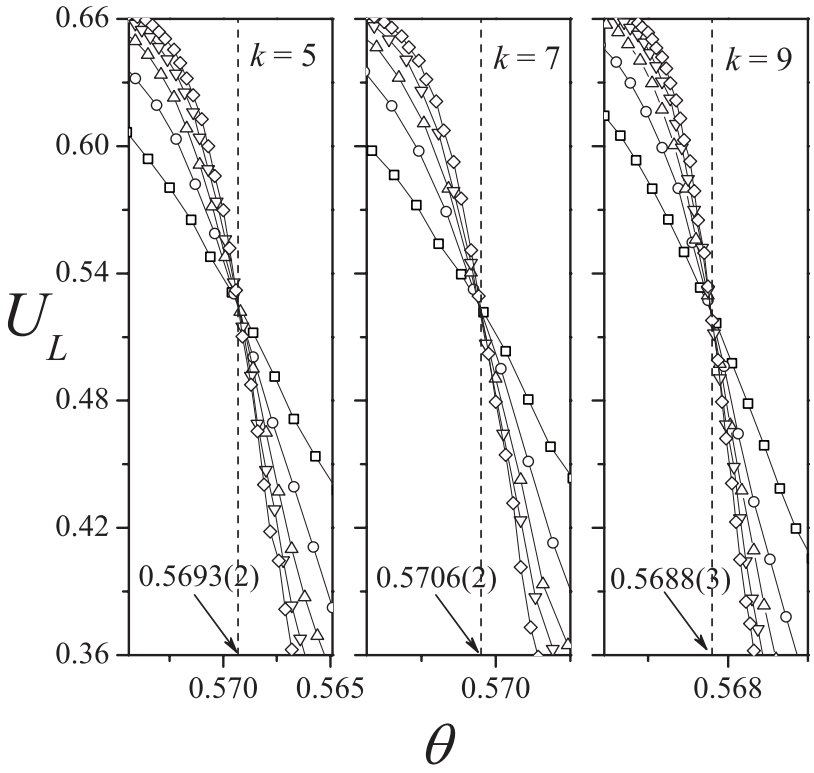

Figure 4. Curves of U_L versus θ for $k = 5$ (left), $k = 7$ (middle) and $k = 9$ (right) and different lattice sizes: $L/k = 128$, squares; $L/k = 256$, circles; $L/k = 384$, up triangles; $L/k = 512$, down triangles and $L/k = 640$, diamonds. From their intersections one obtains the percolation threshold $\theta_{c,k}$ in the thermodynamic limit.

Figure 6 also includes the curve of $\theta_{j,k}$ as a function of k. Open circles correspond to values reported in [30] and the solid line was obtained from equation (1). The region above this curve represents the space of all the allowed values of θ (values of θ which can be reached by removing straight rigid k-mers from the surface). On the other hand, the region below the curve of $\theta_{j,k}$ (indicated by light grey in the figure) corresponds to a forbidden region of the θ-space.

The curve of $\theta_{c,k}$ divides the space of allowed values of θ in a percolating region ($\theta > \theta_{c,k}$) and a non-percolating region ($\theta_{j,k} < \theta < \theta_{c,k}$). These phases extend to infinity in the space of the parameter k (see figure 6(b)) and, consequently, the model presents percolation transition in all the ranges of k. In contrast, when straight rigid k-mers are randomly and irreversibly deposited on a square lattice, the percolation phase transition only exists for values of k ranging between 1 and approximately 1.2×10^4 [11]. For $k > 1.2 \times 10^4$, the predicted value of $\theta_{c,k}$ exceeds the corresponding value of $\theta_{j,k}$ and percolation phase transition is impossible [11].

5. Critical exponents and universality

In this section, the critical exponents ν, β and γ will be calculated. Critical exponents are of importance because they describe the universality class of a system and allow for the understanding of the related phenomena.

J. Stat. Mech. (2015) P09003

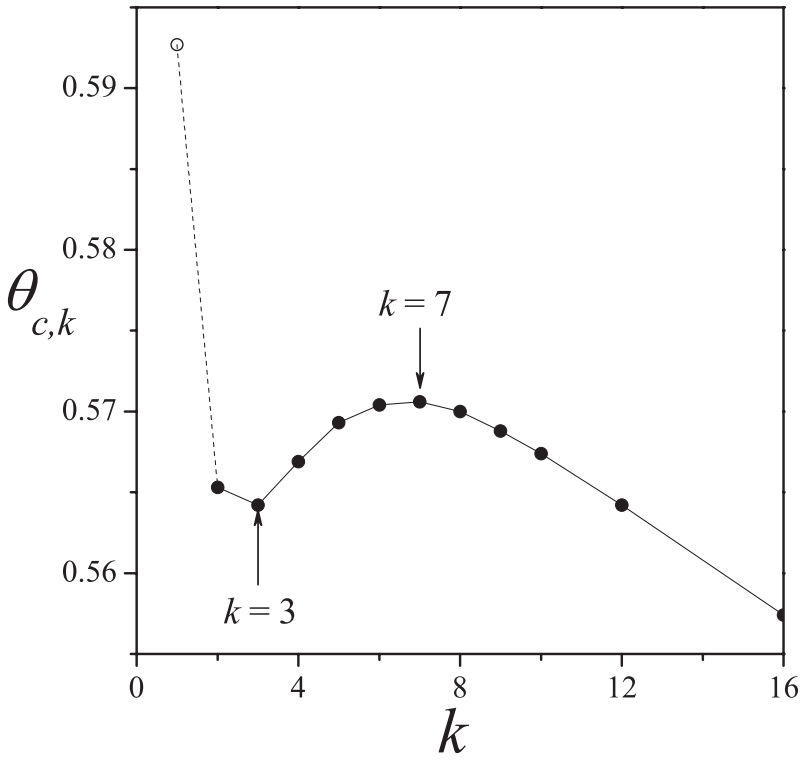

Figure 5. Percolation threshold $\theta_{c,k}$ as a function of k for k ranging between 1 and 16.

Table 1. Compilation of the percolation thresholds for different values of k.

k	$\theta_{c,k}$
2	0.5653(1)
3	0.5642(2)
4	0.5669(1)
5	0.5693(1)
6	0.5704(2)
7	0.5706(1)
8	0.5700(2)
9	0.5688(2)
10	0.5674(1)
12	0.5642(1)
16	0.5574(1)
20	0.551(1)
32	0.536(1)
64	0.513(2)
128	0.491(4)
256	0.470(3)
∞	0.454(4)

The standard theory of finite-size scaling allows for various ways of estimating ν from numerical data. One of these methods is from the maximum of the function in equation (4) [1],

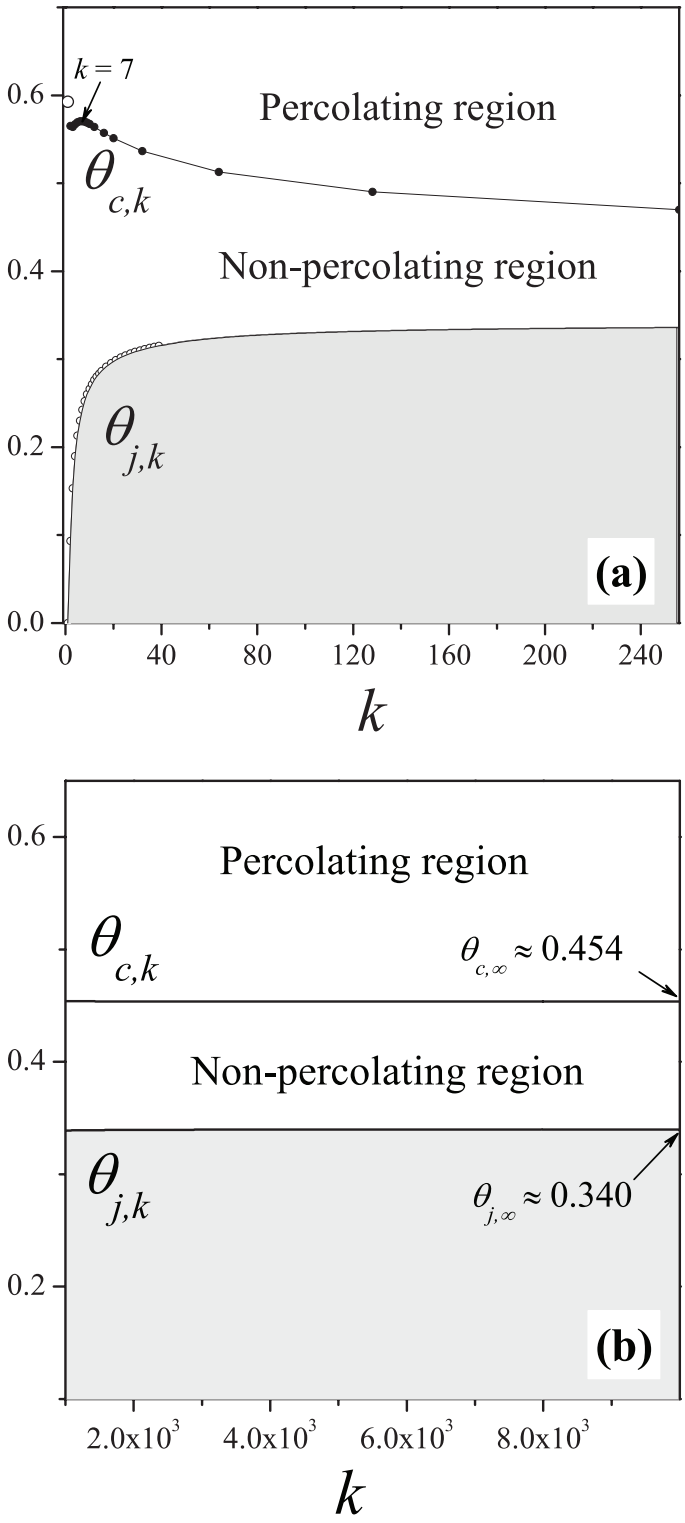

Figure 6. The percolation threshold $\theta_{c,k}$ (solid circles) and limit coverage $\theta_{j,k}$ (open circles) for intermediate (a) and large (b) values k. The results in part (b) correspond to the fitting functions as discussed in the text. The curve of $\theta_{c,k}$ divides the space of allowed values of θ in a percolating region ($\theta > \theta_{c,k}$) and a non-percolating region ($\theta_{j,k} < \theta < \theta_{c,k}$). The region below the curve of $\theta_{j,k}$ (indicated by light grey in the figure) corresponds to a forbidden region of θ-space.

$$\left(\frac{\mathrm{d}R^X_{L,k}}{\mathrm{d}\theta}\right)_{\max} \propto L^{1/\nu}. \tag{6}$$

In figure 7(a), $\ln[(\mathrm{d}R^A_{L,k}/\mathrm{d}\theta)_{\max}]$ has been plotted as a function of $\ln[L]$ (note the log–log functional dependence) for $k = 5$, 7 and 9 as indicated. According to equation (6) the slope of each line corresponds to $1/\nu$. As can be observed, the slopes of the curves remain constant (and close to 3/4) for all studied cases. Thus, $\nu = 1.35(2)$ for $k = 5$; $\nu = 1.32(2)$ for $k = 7$ and $\nu = 1.33(2)$ for $k = 9$. The results coincide, within numerical errors, with the exact value of the critical exponent of the ordinary percolation $\nu = 4/3$.

Another alternative way of evaluating ν is given through the divergence of the root mean square deviation of the threshold observed from their average values, $\Delta^X_{L,k}$ in equation (4) [1],

$$\Delta^X_{L,k} \propto L^{-1/\nu}. \tag{7}$$

The inset in figure 7(a) shows $\ln(\Delta^A_{L,k})$ as a function of $\ln(L)$ (note the log–log functional dependence) for $k = 5$, 7 and 9. According to equation (7), the slope of each line corresponds to $-1/\nu$. As in the main figure, the slopes of the curves remain constant and close to $-3/4$. In this case, $\nu = 1.36(3)$ for $k = 5$; $\nu = 1.31(3)$ for $k = 7$ and $\nu = 1.35(3)$ for $k = 9$.

The procedure in figure 7(a) was repeated for the I and U percolation criteria. Thus, six values of ν were obtained for each value of k. For either equation (6) or equation (7) we can have at least three possible percolation methods: $X = I$, U, A. In all cases, the results coincide, within numerical errors, with the exact value of the critical exponent of the ordinary percolation, namely, $\nu = 4/3$.

Once we know ν, the exponent γ can be determined by scaling the maximum value of the susceptibility equation (2). According to the finite-size scaling theory [1], the behavior of χ at criticality is $\chi = L^{\gamma/\nu}\overline{\chi}(u)$, where $u = (\theta - \theta_c)L^{1/\nu}$ and $\overline{\chi}$ is the corresponding scaling function. At the point where χ is maximal, $u =$ const. and $\chi_{\max} \propto L^{\gamma/\nu}$. Our data for $\chi_{\max}$ is shown in figure 7(b). The values obtained are $\gamma = 2.39(2)$ for $k = 5$; $\gamma = 2.33(6)$ for $k = 7$ and $\gamma = 2.38(2)$ for $k = 9$. The simulation data is consistent with the exact value of the critical exponent of ordinary percolation, $\gamma = 43/18$.

On the other hand, the standard way of extracting the exponent ratio β is to study the scaling behavior of P at criticality [1],

$$P = L^{-\beta/\nu}\overline{P}(u'), \tag{8}$$

where $u' = |\theta - \theta_c|L^{1/\nu}$ and $\overline{P}$ is the scaling function. At the point where $\mathrm{d}P/\mathrm{d}\theta$ is maximal, $u =$ const. and

$$\left(\frac{\mathrm{d}P}{\mathrm{d}\theta}\right)_{\max} = L^{(-\beta/\nu+1/\nu)}\overline{P}(u') \propto L^{(1-\beta)/\nu}. \tag{9}$$

The scaling of $(\mathrm{d}P/\mathrm{d}\theta)_{\max}$ is shown in figure 7(c) for $k = 5$, 7 and 9. From the slopes of the curves, the following values of β were obtained: $\beta = 0.14(1)$ for $k = 5$; $\beta = 0.14(1)$ for $k = 7$ and $\beta = 0.15(2)$ for $k = 9$. These results agree very well with the exact value of β for ordinary percolation, $\beta = 5/36$.

J. Stat. Mech. (2015) P09003

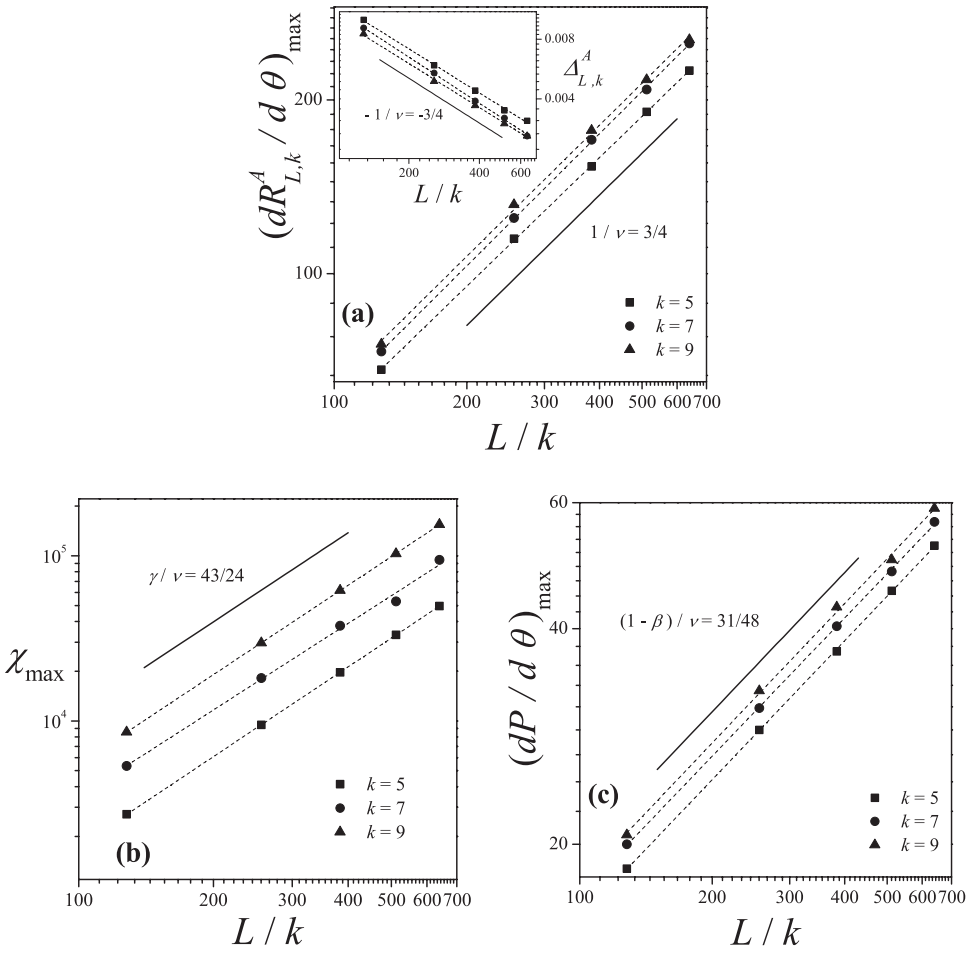

Figure 7. (a) Log–log plot of $(\mathrm{d}R^A_{L,k}/\mathrm{d}\theta)_{\max}$ as a function of L/k for different values of k as indicated. According to equation (6) the slope of each line corresponds to $1/\nu = 3/4$. Inset: $\ln(\Delta^A_{L,k})$ as a function of L/k for $k = 5$ (squares), $k = 7$ (circles) and $k = 9$ (triangles). According to equation (7), the slope of each curve corresponds to $-1/\nu = -3/4$. (b) Log–log plot of $\chi_{\max}$ as a function of L/k for different values of k as indicated. The slope of each line corresponds to $\gamma/\nu = 43/24$. (c) Log–log plot of $(\mathrm{d}P/\mathrm{d}\theta)_{\max}$ as a function of L/k for different values of k as indicated. According to equation (9), the slope of each curve corresponds to $(1-\beta)/\nu = 31/48$.

The values calculated for ν (figure 7(a)), γ (figure 7(b)) and β (figure 7(c)) clearly indicate that this problem belongs to the same universality class as random percolation regardless of the size of k considered.

Scaling behavior can be further tested by plotting $R^X_{L,k}(\theta)$ versus $(\theta - \theta_{c,k})L^{1/\nu}$, $PL^{\beta/\nu}$ versus $|\theta - \theta_{c,k}|L^{1/\nu}$ and $\chi L^{-\gamma/\nu}$ versus $(\theta - \theta_{c,k})L^{1/\nu}$ and looking for data collapsing [1]. Using the values of θ_c calculated above and the exact values of the critical exponents of ordinary percolation $\nu = 4/3$, $\beta = 5/36$ and $\gamma = 43/18$, we obtain an excellent scaling collapse as shown in figures 8 and 9 for for $k = 5$, 7 and 9 as indicated. This leads to independent controls and consistency checks of the values of all the critical exponents.

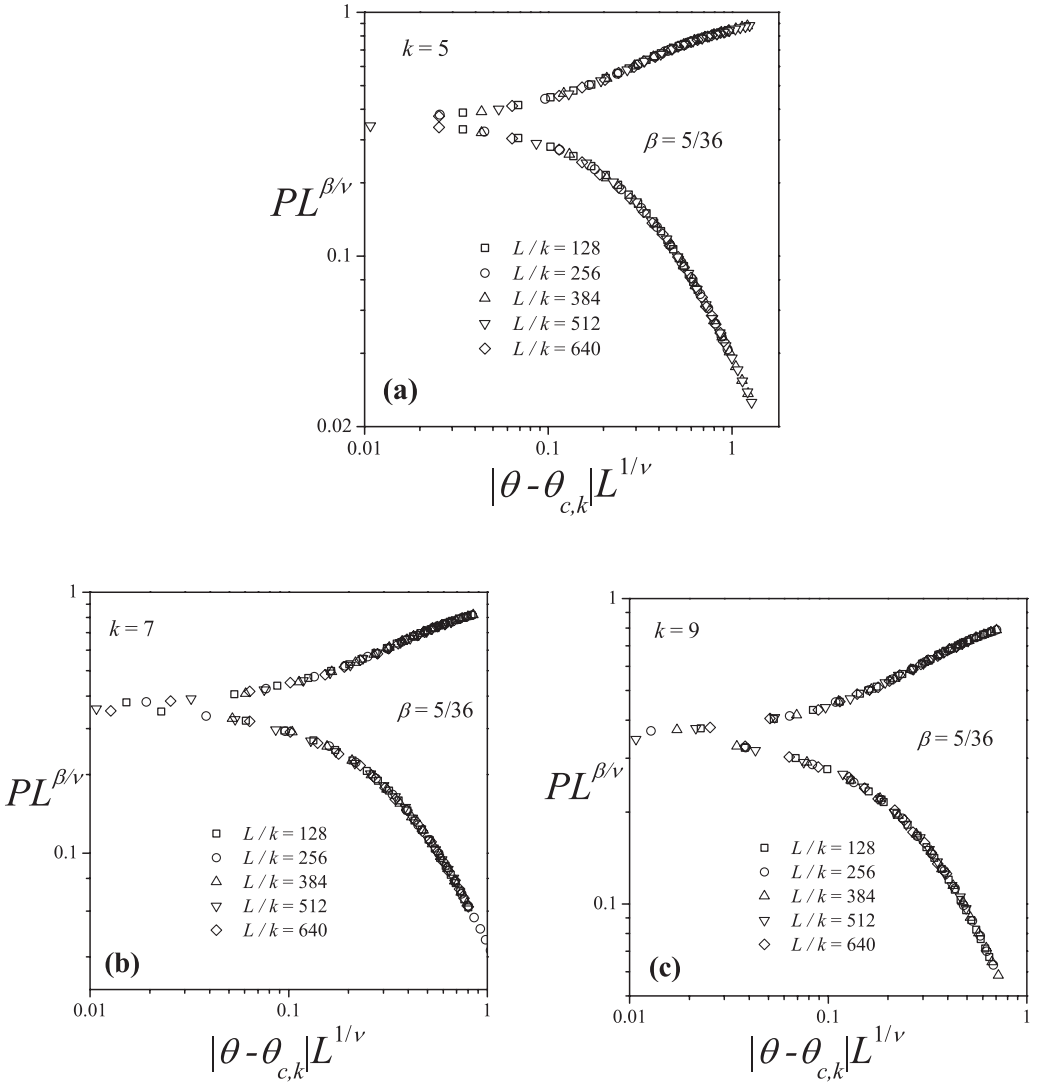

Figure 8. Data collapsing of the percolation order parameter, $PL^{\beta/\nu}$ versus $|\theta - \theta_{c,k}|L^{1/\nu}$, for $k = 5$ (a), $k = 7$ (b) and $k = 9$ (c). The plots were made using $\theta_{c,k=5} = 0.5693$, $\theta_{c,k=7} = 0.5706$, $\theta_{c,k=9} = 0.5688$ and the exact percolation exponents $\nu = 4/3$ and $\beta = 5/36$.

6. Conclusions

The problem of inverse percolation by removing straight rigid rods from square lattices has been studied by numerical simulations and finite-size analysis. The process starts with an initial configuration, where all lattice sites are occupied and, obviously, the opposite sides of the lattice are connected by occupied sites. Then, the system is diluted by randomly removing straight rigid rods of length k (k-mers) from the surface.

The percolation phase occurring at high concentrations is separated from a non-percolation phase by a continuous transition occurring at an intermediate critical density $\theta_{c,k}$. This critical density was calculated as a function of k. The results, obtained for k ranging from 2 to 256, showed a nonmonotonic size k dependence for $\theta_{c,k}$, which rapidly

J. Stat. Mech. (2015) P09003

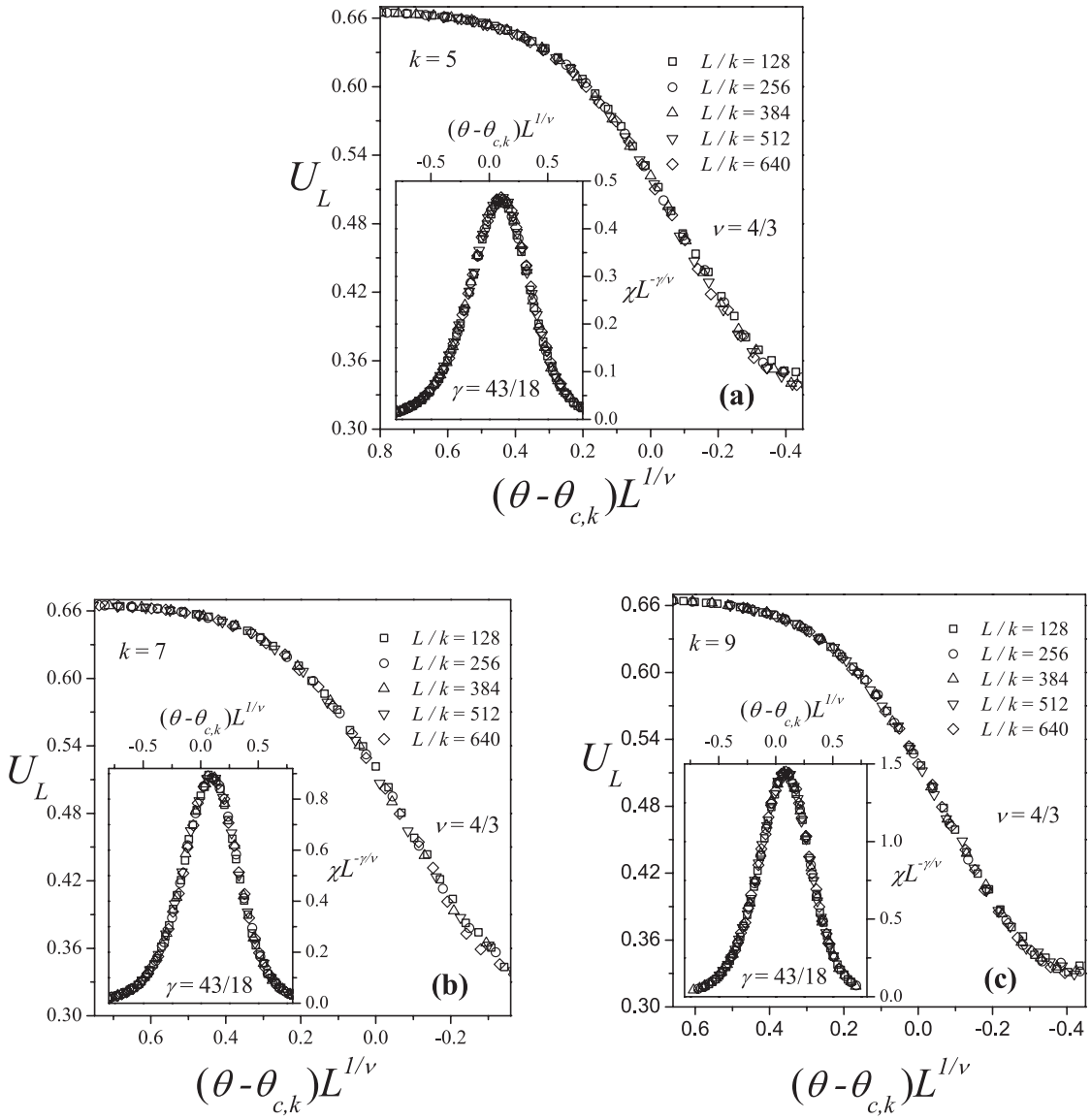

Figure 9. Data collapsing of the cumulant, U_L versus $(\theta - \theta_{c,k})L^{1/\nu}$, and of the susceptibility, $\chi L^{-\gamma/\nu}$ versus $(\theta - \theta_{c,k})L^{1/\nu}$ (inset), for $k = 5$ (a), $k = 7$ (b) and $k = 9$ (c). The plots were made using $\theta_{c,k=5} = 0.5693$, $\theta_{c,k=7} = 0.5706$, $\theta_{c,k=9} = 0.5688$ and the exact percolation exponents $\nu = 4/3$ and $\gamma = 43/18$.

decreases for small particle sizes ($1 \leqslant k \leqslant 3$). Then, it grows for $k = 4$, 5 and 6, goes through a maximum at $k = 7$, and finally decreases again and asymptotically converges towards a definite value for large values of k ($\theta_{c,\infty} = 0.454(4)$).

Percolating and non-percolating phases extend to infinity in the parameter space k and, consequently, the model presents percolation transition in all ranges of k-mer size. This situation contrasts with the complementary case of the deposition of straight rigid k-mers on square lattices, where percolation phase transition only exists for values of k ranging between 1 and approximately 1.2×10^4 [11]. For $k > 1.2 \times 10^4$, the predicted value of $\theta_{c,k}$ exceeds the corresponding jamming value $\theta_{j,k}$ and percolation phase

transition is impossible [11]. The main source for this asymmetric behavior is the breaking of particle-hole symmetry occurring for $k \geqslant 2$.

As is standard in the literature [11], our predictions for infinitely large k-mers are based on simulation results obtained for not very large particles (in this case $2 \leqslant k \leqslant 256$) and then extrapolated to represent very long objects. Future efforts will focus on the development of more extensive simulations, which are necessary for obtaining a direct confirmation of the behavior of threshold limits.

Finally, the accurate evaluation of the complete set of static critical exponents ν, β and γ, revealed that the model considered here belongs to the same universality class as random percolation regardless of the value of k considered.

Acknowledgments

This work was supported in part by CONICET (Argentina) under project number PIP 112-201101-00615; Universidad Nacional de San Luis (Argentina) under project 322000; and the National Agency of Scientific and Technological Promotion (Argentina) under project PICT-2013-1678. The numerical work was done using the BACO parallel cluster (composed by 70 PCs each with an Intel i7-3370/2600 processor) located at Instituto de Física Aplicada, Universidad Nacional de San Luis—CONICET, San Luis, Argentina.

References

[1] Stauffer D and Aharony A 1994 *Introduction to Percolation Theory* (London: Taylor and Francis)
[2] Sahimi M 1994 *Applications of Percolation* (London: Taylor and Francis)
[3] Bollobás B and Riordan O 2006 *Percolation* (Cambridge: Cambridge University Press)
[4] Shao J, Havlin S and Stanley H E 2009 *Phys. Rev. Lett.* **103** 018701
[5] Goldenberg J, Libai B, Solomon S, Jan N and Stauffer D 2000 *Physica* A **284** 335
[6] Becklehimer J and Pandey R B 1992 *Physica* A **187** 71
[7] Cornette V, Ramirez-Pastor A J and Nieto F 2003 *Physica* A **327** 71
[8] Cornette V, Ramirez-Pastor A J and Nieto F 2003 *Eur. Phys. J.* B **36** 391
[9] Leroyer Y and Pommiers E 1994 *Phys. Rev.* B **50** 2795
[10] Kondrat G and Pękalski A 2001 *Phys. Rev.* E **63** 051108
[11] Tarasevich Y Y, Lebovka N I and Laptev V V 2012 *Phys. Rev.* E **86** 061116
[12] Newman M, Barabási A-L and Watts D J 2006 *The Structure and Dynamics of Networks* (Princeton, NJ: Princeton University Press)
[13] Dorogovtsev S N and Mendes J F F 2003 *Evolution of Networks: from Biological Nets to the Internet and WWW* (Oxford: Oxford University Press)
[14] Kerstein A R 1983 *J. Phys. A: Math. Gen.* **16** 3071
[15] Rintoul M D 2000 *Phys. Rev.* E **62** 68
[16] Klemm A, Kimmich R and Weber M 2001 *Phys. Rev.* E **63** 041514
[17] Yi Y B 2006 *Phys. Rev.* E **74** 031112
[18] Yi Y B and Esmail K 2011 *J. Appl. Phys.* **111** 124903
[19] Sole V R and Jose M M 2001 *Proc. R. Soc.* B **268** 2039
[20] Motter A, Gulbahce N, Almaas E and Barabási A-L 2008 *Mol. Syst. Biol.* **4** 168
[21] Albert R, Jeong H and Barabási A-L 2000 *Nature* **406** 378
[22] Albert R and Barabási A-L 2002 *Rev. Mod. Phys.* **74** 47
[23] Hinrichsen H 2000 *Adv. Phys.* **49** 815
[24] Krapivsky P L, Redner S and Naim E B 2010 *A Kinetic View of Statistical Physics* (Cambridge: Cambridge University Press)
[25] Evans J W 1993 *Rev. Mod. Phys.* **65** 1281
[26] Bonnier B, Hontebeyrie M, Leroyer Y, Meyers C and Pommiers E 1994 *Phys. Rev.* E **49** 305
[27] Lebovka N I, Karmazina N N, Tarasevich Y Y and Laptev V V 2011 *Phys. Rev.* E **84** 061603

J. Stat. Mech. (2015) P09003

[28] Longone P, Centres P M and Ramirez-Pastor A J 2012 *Phys. Rev.* E **85** 011108
[29] Privman V and Nielaba P 1992 *Europhys. Lett.* **18** 673
[30] Dolz M, Nieto F and Ramirez-Pastor A J 2005 *Phys. Rev.* E **72** 066129
[31] Hoshen J and Kopelman R 1976 *Phys. Rev.* B **14** 3428
[32] Yonezawa F, Sakamoto S and Hori M 1989 *Phys. Rev.* B **40** 636
[33] Binder K 1997 *Rep. Prog. Phys.* **60** 488
[34] Biswas S, Kundu A and Chandra A K 2011 *Phys. Rev.* E **83** 021109
[35] Chandra A K 2012 *Phys. Rev.* E **85** 021149
[36] Cardy J 1992 *J. Phys. A: Math. Gen.* **25** L201
[37] Watts G M T 1996 *J. Phys. A: Math. Gen.* **29** L363
[38] Simmons J J H, Kleban P and Ziff R M 2007 *J. Phys. A: Math. Gen.* **40** F771
[39] Ziff R M and Newman M E J 2002 *Phys. Rev.* E **66** 016129
[40] Lee M J 2008 *Phys. Rev.* E **78** 031131

J. Stat. Mech. (2015) P09003